Bulletin of Glacier Research 7 (1989) 89–98

Characteristics of heat and water fluxes on glacier and ground surfaces in the West Kunlun Mountains

Shuhei TAKAHASHI[1], Tetsuo OHATA[2] and XIE Yingqin[3]

1 Kitami Institute of Technology, Kitami 090 Japan

2 Water Research Institute, Nagoya University, Nagoya, 464 Japan

3 Lanzhou Institute of Glaciology and Geocryology, Academia Sinica, Lanzhou, China

(Received December 9, 1988; Revised manuscript received January 29, 1989)

Abstract

The heat and water balances were examined at the Chongce Ice Cap and its surroundings in summer, 1987. On a glacier surface at the terminus of the ice cap (5850m a.s.l.), the latent heat loss by evaporation was much larger than the heat used for snow melting. The evaporation from the surface was the main component for the outgoing mass flux. The evaporation rate was correlated with air temperature, and estimated as 1.36mm/d between July 23 and August 18. The melting rate was correlated with solar radiation, and estimated as 3.52mm/d. On a ground surface (5260m a.s.l.), the amount of evaporation (51.6mm, between July 17 and August 22) was almost equal to that of precipitation (52.3mm); no water was percolated into the ground. The large evaporation rate is considered to be owing to the arid climate, the low atmospheric pressure at high altitude, and the strong solar radiation in this area.

1. Introduction

The West Kunlun Mountains are located in the arid climate region between the Taklimakan Desert and Tibet Highland. Because of the small precipitation, the snow line is very high in this area, generally 5700–6120m (Zhang and Jiao, 1986). On the glaciers at high altitudes in this area, the evaporation from the surface should be large because of the arid climate and the low atmospheric pressure (below 500mb). Consequently, the heat balance and water balance should be different from other areas. These heat and water balances are important to know the mechanism of glacier formation and the water circulation in the arid climate area.

In the summer season of 1987, to examine the characteristics of the heat and water balances, meteorological, hydrological and glaciological observation were carried out on the Chongce Ice Cap in the West Kunlun Mountains in China and the surrounded ground surface.

2. Outline of observations

The Chongce Ice Cap is located at 35°14'N, 81°07'E in the West Kunlun Mountains, with the altitudes of 6374m at the top and 5750m at the terminus of the glacier. Along a line from the top of the Ice Cap to the shore of Gozha Lake (Fig. 1), components of the heat and the water balances were observed mainly at five stations:

- No. 12 (6327m) near the top of the Ice Cap;
- No. 1 (5850m) at the terminus of Chongce Ice Cap;
- ABC (5805m) on a moraine field;
- BC (5260m) on a bare ground;
- LS (5125m) on the shore of the Gozha Lake.

The same observations were temporarily carried out at No. 8 (6130m) on the Ice Cap, and CG (5500m) in the ablation area of Chongce Glacier.

The observed meteorological and glaciological components at each station are shown in Fig. 2. Digital data recorders were used for the logging of the measured values: temperature; humidity; radiation;

wind speed; wind direction; and air pressure. The recording interval was 10 minutes at BC and No. 12, and 20 minutes at ABC and No. 1. Manually observed elements were evaporation rate on a surface, melting rate on a glacier surface, precipitation, and visual observation of clouds.

Chinese Standard Time (CST), used in this report, is GMT plus 8 hours. Therefore, the solar noon is at about 14h 40m (CST) at the longitude of about 80°E.

We discuss the heat and water fluxes mainly at No. 1 and BC in this report, among the other observations at the five stations.

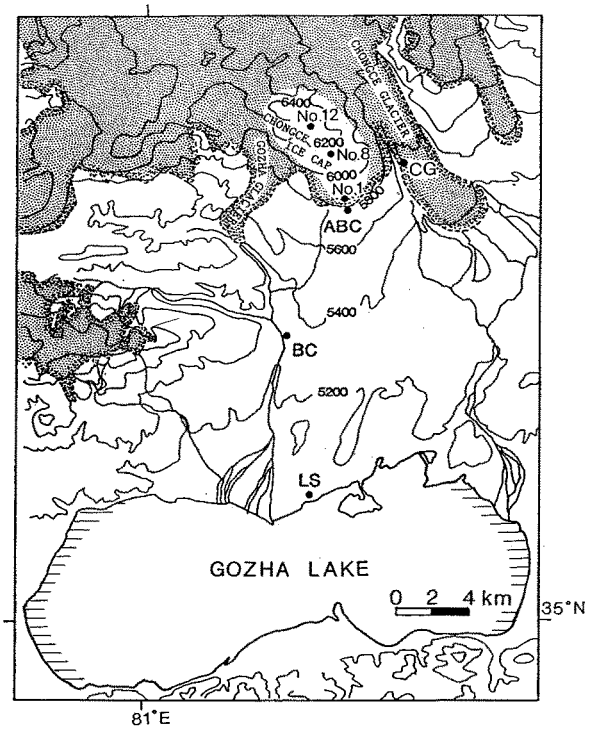

Fig. 1. Location of meteorological stations around Chongce Ice Cap, in the West Kunlun Mountains: LS (5125m), BC (5260m), CG (5500m), ABC (5805m), No. 1 (5850m), No. 8 (6118m) and No. 12 (6327m).

3. Heat and water fluxes on a glacier surface

3.1. Melting rate

Melting rate on the glacier surface was measured by several methods during July 30 – August 2 and August 12 – 18 at No. 1 station on the Chongce Ice Cap (5,850m) and on August 22 – 23 at CG (5500m).

The first method was the snow lysimeter method. The lysimeter was a 0.50m × 0.46m transparent acrylic glass plate with a rim of 2cm high. It was

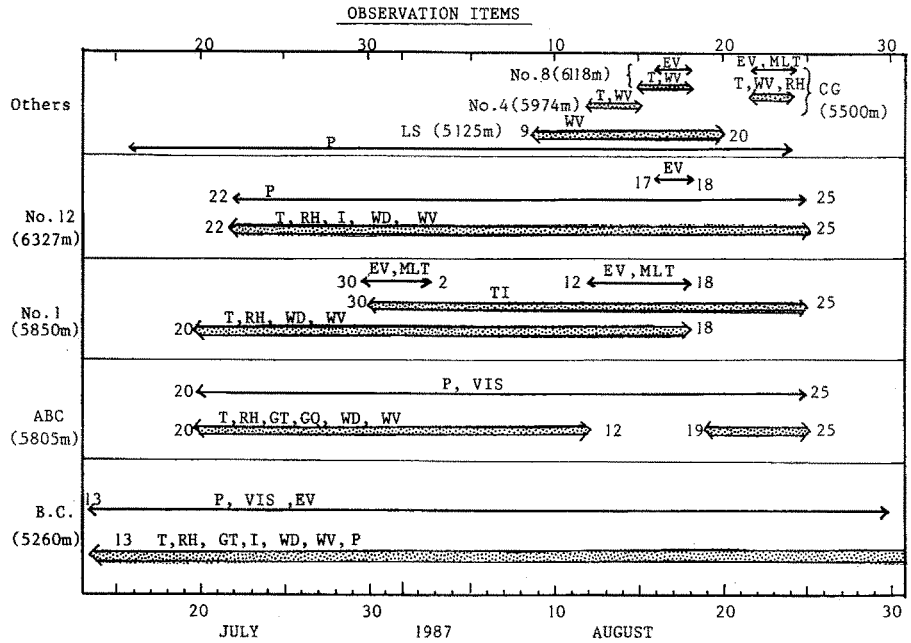

Fig. 2. Observation period and observed meteorological and glaciological components for each station. T: temperature, TI: ice temperature, RH: relative humidity, WD: wind direction, WV: wind speed, GT: ground temperature, GQ: geo-heat flux, P: precipitation, EV: evaporation, MLT: melting amount, VIS: cloud amount.

installed 10cm below the snow surface. Since the lysimeter was set tilted, melt water dripped from its corner and was stored in a bottle (Fig. 3a). The stored water was weighed at intervals of 1 or 2 hours.

Another method was the snow stake method. It has a problem: a hollow around the snow stale was formed in a few days after the setting of the snow stake due to the strong solar radiation reflected from the stake. It made the measurement of surface level difficult. To prevent this problem, a strained string with several marks was spanned between two stakes, and the heights of the marks from the snow surface were measured (Fig. 3b). This method worked well in several days, but, as the stakes tilted due to the hollow around it, the heights did not show correct values. To prevent this error, another type of stake was prepared: a stake with four horizontal sticks (Fig. 3c). When the stake was tilted, the height changes of the stick at one side to another side are opposite, and the changes due to the stake tilting are canceled out each other when they are averaged.

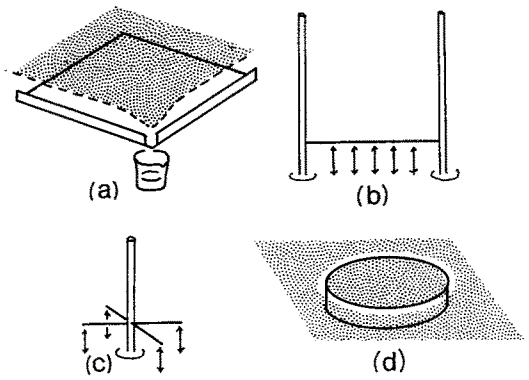

Fig. 3. Methods for melting rate observation. (a) lysimeter, (b) two stakes with a strained string, (c) stake with four horizontal sticks, (d) evaporation pan in which melt water was weighed.

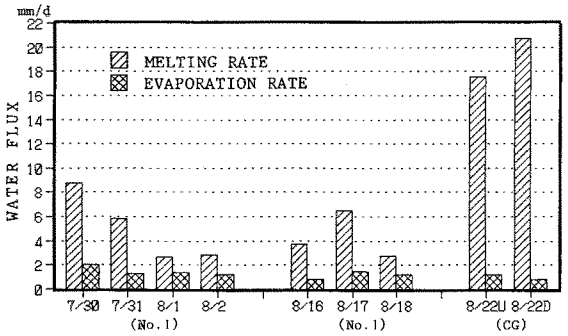

Fig. 4. Melting rate and evaporation rate at No. 1 from July 30 to August 18, and at CG (5500m) on August 22 (U: on the top of undulation, D: on the bottom).

The third method was by weighing the melt water in the evaporation pan. During the evaporation measurement, the snow in the pan was occasionally reset when the snow contained much melt water. At the time of resetting, the snow was weighed before and after draining the melt water to obtain the amount of the drained water. As the melt water cannot be drained completely, the drained water does not exactly indicate the melt water amount. Compared with the lysimeter measurement, the snow after draining was found to contain about 15% residual water of by weight. Thus, the amount of the melt water was roughly obtained by adding this residual water amount to the amount of drained water.

Among the above-described methods, an adequate method was adopted for the melting rate measurement according to the surface condition. The results at No. 1 and CG are shown in Fig. 4. The melting occurred only in daytime usually from 12h to 19h. The daily total of the melt on fine days at No. 1 was ranged from 3 to 9mm, whereas it was about 20mm at CG.

3.2. Evaporation rate on a glacier surface

Evaporation rate on the glacier surface was obtained in daytime as a change in weight of snow in an evaporation pan (an acrylic glass pan with 23cm diameter and 3cm depth) at an interval of 1 or 2 hours. Evaporation rate in nighttime was measured once from 20h to 8h the next morning. Two pans were used for the measurement to compare with each other; usually they showed the same results. When melt water appeared at the bottom of the pan, the snow in the pan was reset, usually once in a day.

The observed daily evaporation rate is shown in Fig. 4. The average of evaporation rate at No. 1 was 1.46mm/d from July 30 to August 2, and 1.18mm/d from August 16 to 18. The evaporation rate had a large diurnal variation (Fig. 5). The variation was large in daytime (during melting time), and the maximum rate was ranging from 3 to 7mm/d. The nighttime evaporation (exactly speaking, it was sublimation because the surface was frozen) was quite small or negligible, less than about 0.5mm/d.

The evaporation rate varied with altitude. From August 17 to August 18, the evaporation rate was measured simultaneously at No. 1, No. 8 and No. 12,

all on the ice cap. The evaporation rate decreased with altitude:

1.86mm/d (100%) at No. 1 (5850m),
1.37mm/d (74%) at No. 8 (6130m),
and 0.97mm/d (52%) at No. 12 (6237m).

This dependence of evaporation rate on altitude can be explained by the difference of length of melting time as follows. The melting time on the ice cap was limited in daytime as seen in the water content observation (Fig. 6). Evaporation rate is large in the melting time as mentioned above, and the melting time in a day would decrease with altitude as air temperature decreases with altitude (the temperature at No. 12 was −3°C lower than No. 1). Thus, the evaporation decreases with altitude.

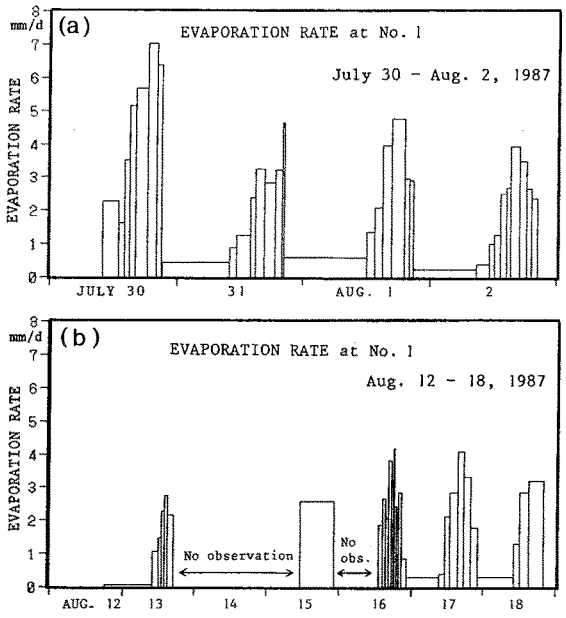

Fig. 5. Diurnal variation of evaporation rate at No. 1.
(a): between July 30 and August 2, (b): between August 12 and 18, 1987.

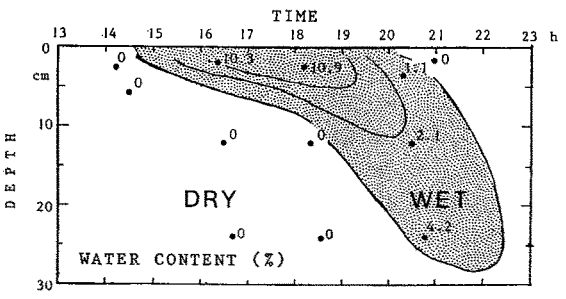

Fig. 6. Diurnal variation of water content (%) in snow layers at No. 8 (6118m) on August 17, 1987.

3.3. *Albedo and short wave radiation*

Albedo, the ratio of the reflective radiation to the global solar radiation, was measured at No. 1 from July 23 to August 18 at intervals of 20 minutes, by two photo-diode sensors (Silicon photo-diode; Hamamatsu Photonics Co., S875-66R) which is horizontally mounted at the height of 1m from the surface. The sensors were attached to the upper and the lower side of rectangular column with a cross section of 2cm × 2cm. The detectable wavelength of the sensors was between 430 nm and 1060 nm. Since the reflectivity of a snow surface depends on wave length, the albedo observation by the photo-diode sensors has some error by its dependency on wave length.

At No. 12 (5km far from No. 1), global radiation was measured by a global radiometer (Aanderaa Co., No. 2770; detectable wavelength: between 300 and 2500nm). Global radiation at No.1 was assumed to be the same as that at No. 12. From the global radiation, I, and the albedo, A, the net short-wave radiation at No. 1, Q_{RS}, was obtained as $(1-A)I$.

The variation of albedo, solar radiation, and net short-wave radiation on a glacier surface are shown in Fig. 7. The albedo at first had the high values of 0.8 to 0.9 until July 29; subsequently it gradually decreased to about 0.4 on August 1. This decrease in albedo was caused by melt water which overflowed on the surface and refroze at night, forming a bare ice surface. From August 3, the surface was covered with new snow, and the albedo showed a high value again. The global radiation, I, was large on fine days, about 38 MJ/m² at the end of July. The net short-wave radiations, Q_{RS}, were large, about 14 MJ/m²d, on August 1 and 2 owing to the small albedos.

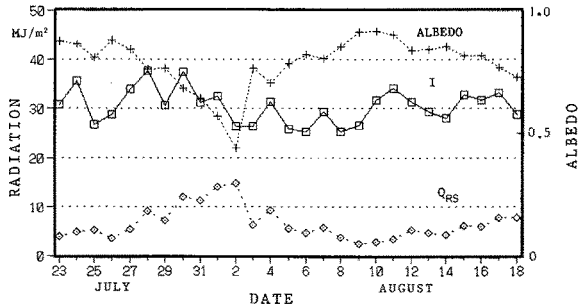

Fig. 7. Solar radiation (I), albedo and net short-wave radiation (Q_{RS}) at No. 1.

3.4. *Heat balance and water balance on a glacier surface*

Heat fluxes to the glacier surface are balanced as follows:

$$Q_{NR}+Q_S+Q_L+Q_M+Q_C=0, \quad (1)$$

where Q_{NR} is the net radiation, Q_S the sensible heat flux, Q_L the latent heat flux, Q_M the heat for snow melting, and Q_C the conductive heat flux from the subsurface to the surface. Q_{NR} is the net sum of the net short-wave radiation, Q_{RS}, and the net long-wave radiation, Q_{RL}, and expressed as:

$$Q_{NR}=Q_{RS}+Q_{RL} \quad (2)$$

$$=I(1-A)+Q_{RL}\downarrow+Q_{RL}\uparrow, \quad (3)$$

where $Q_{RL}\downarrow$ and $Q_{RL}\uparrow$ are the downward (atmospheric) and upward (terrestrial) long wave radiation.

In the observation period on Chongce Ice Cap, meteorological factors (temperature, humidity, wind speed, wind direction, solar radiation and albedo) were continuously recorded by data recorders, whereas evaporation rate for Q_L and melting rate for Q_M were occasionally obtained by manual measurements.

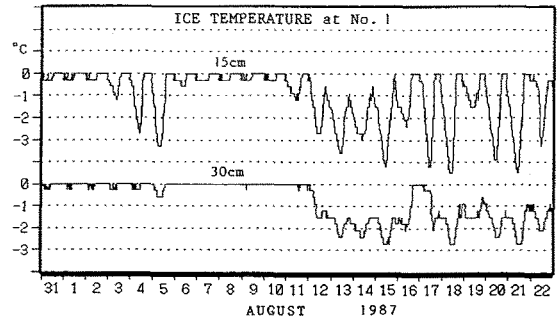

Fig. 8. Ice temperatures at depths of 15cm and 30cm at No. 1.

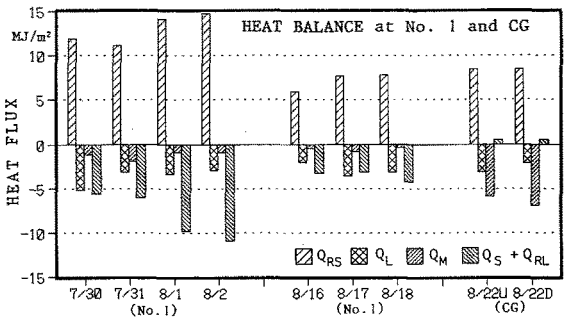

Fig. 9. Heat balance on a glacier surface at No. 1. from July 30 to August 18, and at CG (5500m) on August 22 (U: on the top of undulation, D: on the bottom).

Ice temperatures at 15cm deep and at 30cm deep were shown in Fig. 8. Due to the solar radiation and the space which appeared between the ice and the sensor, the measured temperature was sometimes positive in daytime. The positive temperature is not the real ice temperature, and assumed as 0°C in Fig. 8. Before August 11, the ice temperatures at the two depths were almost 0°C; therefore Q_C was zero. After August 12, the temperatures at 30cm deep decreased to about −1.5°C. However, the sign of difference in the ice temperatures between 15cm and 30cm deep was opposite from daytime to nighttime; therefore the Q_C can also be neglected.

Due to troubles in the net radiation sensor, long-wave radiation was not observed on the glacier surface. The sensible heat, Q_S, was also difficult to obtain. Since the surface temperature was not measured and the eddy diffusivity at sea level would not apply at this altitude where the atmospheric pressure was lower than 500 mb, the bulk method for the sensible heat flux could not be applied to estimate Q_S. So, the sum of the heat fluxes Q_S and Q_{RL} was obtained as a residue of the other heat fluxes by equation (1):

$$Q_S+Q_{RL}=-(I(1-A)+Q_M+Q_L). \quad (4)$$

In Fig. 9, the occasional observations of these heat fluxes at No. 1 are shown from July 30 to August 18, and at CG (5500m) on August 22. At No. 1, Q_{RS} was the only heat source and the others were the heat sinks. In the heat sinks, the latent heat flux, Q_L, was much larger than the heat for melting, Q_M, and the sum Q_S+Q_{RL} was a larger heat loss. These were attributed to the low daily mean temperature of below 0°C, by which Q_M, Q_S and Q_{RL} tend to be small or negative. At CG, Q_M was the largest heat sink and $Q_{RL}+Q_S$ was small and positive. It was due to the higher air temperatures than those at No. 1 because the altitude at CG was 300m lower than at No. 1.

3.5. *Water flux from a glacier surface*

On the Ice Cap surface, the outgoing water fluxes were melting and evaporation, while the incoming was mainly precipitation. The net water flux should be balanced with the divergence of glacier mass flow in equilibrium over a long period.

Precipitation during the observation period from July 19 to August 25 at No. 1 can be estimated as about 130mm (Ohata *et al*, 1989). However, melting and evaporation were occasionally observed, and the

total surface water flux during the period of precipitation observation can be estimated from meteorological factors.

The evaporation showed a better correlation with air temperature as shown in Fig. 10, rather than with vapor pressure and wind speed. This means that the evaporation rate should be large during the melting period in daytime, and the length of the melting period in turn is dependent on air temperature, as described in section 3.2. From the recursive relation between evaporation and temperature, the evaporation rate during the observation period was roughly estimated; the daily average between July 23 and August 18 was 1.36mm/d (Fig. 11).

The melting rate was better correlated with solar radiation as shown in Fig. 12, rather than with air temperature. This tendency can be explained as follows. When the temperature was much higher than 0 °C, the sensible heat flux, Q_S, which linearly depends on air temperature, became a large positive component in the heat balance, and melting rate was better correlated with air temperature. However, on this Ice Cap, the daily average temperature was below 0°C. Therefore, the sensible heat flux, Q_S, was not a main component but net short-wave radiation Q_{RS} played a major role in melting. From the recursive relation between the melting and solar radiation (Fig. 12), the melting during the observation period was roughly estimated; the daily average between July 23 and August 18 was 3.52mm/d (Fig. 11).

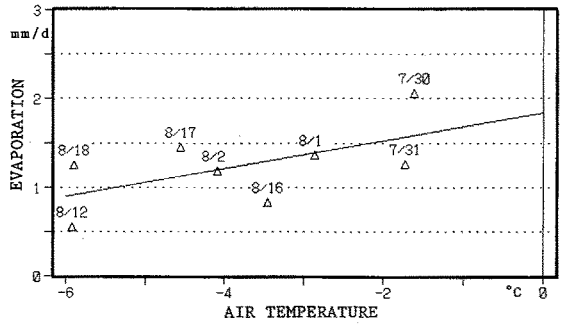

Fig. 10. Relation between evaporation rate and temperature at No. 1.

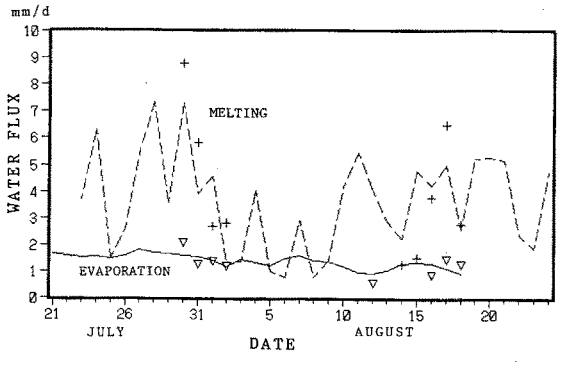

Fig. 11. Estimated melting rate (dashed line) and evaporation rate (solid line). Crosses are observed melting rate and triangles are observed evaporation rates.

Between July 19 and August 25, precipitation was 51 mm at BC and was estimated as 72mm at No.1; the ratio, 1.41, is based on the observations at BC and ABC (5805m a.s.l., near No. 1) (Ohata *et al.*, 1989). During the precipitation observation period, the total evaporation was estimated as 52mm and the total melting was 134mm. The sum of the two outgoing fluxes, which amounts to 186mm, exceeded the precipitation by about 110mm at No. 1. This excess is considered to be the possible ablation at the terminus of the Ice Cap (at No. 1). This ablation estimation was larger than the result of snow stake observation at the upper point 200 m distant from No. 1 (Ageta *et al.*, 1989): the surface lowering of 11cm (40mm water equivalent) between July 19 and August 26. The reason can be in the small albedo due to the overflowed melt-water on the surface which froze at night and formed a bare-ice surface at our observation point.

For the whole Ice Cap, the dependence of water fluxes on altitude will be considered next. The precipitation increased with altitude; at No. 12 (6327m) it was 1.26 times the precipitation at ABC (5850m) (Ohata *et al.*, 1989). On the other hand, the melting rate should decrease with altitude depending on the decrease in air temperature. The evaporation rate also decreases with altitude; evaporation at No. 12 was half of that at No. 1. Therefore, the net accumula-

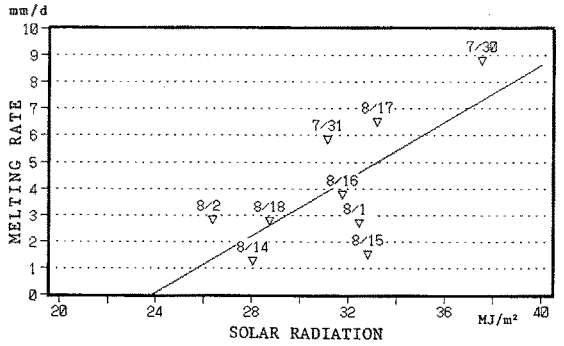

Fig. 12. Relation between melting rate and solar radiation at No. 1.

tion would be positive on the upper part of the Ice Cap.

At high altitudes where ice temperature gets below 0°C, melt water should be re-frozen in the cold layer and form the super-imposed ice; therefore, the melt water would not flow out from the Ice Cap (as shown in Fig. 6). The evaporation/sublimation occurs at all altitudes, (although its rate decreases with altitude), and may occur in all seasons. Consequently, the Chongce Ice Cap is fed by precipitation, and ablated mainly by evaporation not by melting.

4. Heat and water fluxes on a ground surface

The water and heat balance on a ground surface was observed at BC (5260m) from July 17 to August 22. On a few days at the end of July, no data was obtained due to instrument trouble. The surface condition at BC was ground surface with sparse grass. Since the vegetation density at BC was low, any special attentions were not paid to evapotranspiration from the vegetation in the present work. During the observation period, the mean values of meteorological elements were as follows. Air temperature: 3.0°C; relative humidity: 66%; wind speed: 2.9 m/s; daily global radiation: 26.0 MJ/m² (619 ly); cloud amount: 6.7. Precipitation was all snow; 64% of it occurred at night (20–08h).

The water balance, discriminating between the solid form (snow) and liquid form (rain) at the surface, can be written as follows.

$$P+E+R=0 \qquad (5)$$
$$P=P_s+P_l$$
$$E=E_s+E_l$$

where

P: Total precipitation,
E: Sum of sublimation and evaporation,
P_s, P_l: Amounts of solid and liquid phase precipitation,
E_s, E_l: Sublimation and evaporation,
R: Water flux to the subsurface.

The heat balance can be written in the same form as eq. (1). Each component was independently observed except Q_S. Q_S was derived as a residue of the heat balance equation (eq.(1)).

The following results were obtained for the water and heat balances. In Fig. 13, daily (20–20h) P and E are shown. The precipitation, P, was large in July, but

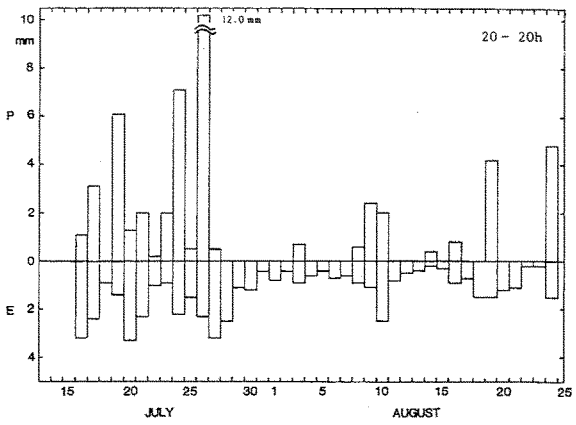

Fig. 13. Precipitation and evaporation on a ground surface at BC (5260m).

it decreased in August. The number of precipitation days was 73% of the whole period (27 days out of 37 days). Maximum intensity of precipitation was 10.4mm/d. Evaporation occurred every day; it was large on days of large precipitation and the succeeding days. This was clearly observed in the period from July 27 to August 1. The total amounts of P and E for the whole period were 52.3 and 51.6mm, respectively. The evaporation rate was 1.36mm/d, which was the same as that at No. 1 (the coincidence in the value to two places of decimals is an accident). The precipitation, P, was roughly balanced by the evaporation, E, for the whole period, resulting in $R=0$. This means that, as a mean for the whole period, all of the precipitation evaporated and no water was percolated into the ground.

The daily heat balance for the period is shown in Fig. 14. The main heat source was Q_{NR}. The heat sink components varied day by day. Q_C and Q_M were small, and Q_C was the larger value when Q_M was large. This means that on snowy days, heat contained in the ground was transported to the surface. The two main heat sink components were Q_L and Q_S. On the large Q_L days, Q_S was small. It can be said that the amounts of Q_L and Q_S were determined by the moisture content of the soil. Large variation in the soil moisture content affected the day-to-day variation in the heat sink components. The total average values of each heat balance component and their ratios to the net radiation are as follows: $Q_{NR}=10.5$ MJ/m²d (100%), $Q_S=-7{,}27$ MJ/m²d (−69%), $Q_L=-2.6$MJ/m²d (−25%), $Q_C=-0.27$ MJ/m²d (−3%), $Q_M=-0.33$ MJ/m²d (−3%).

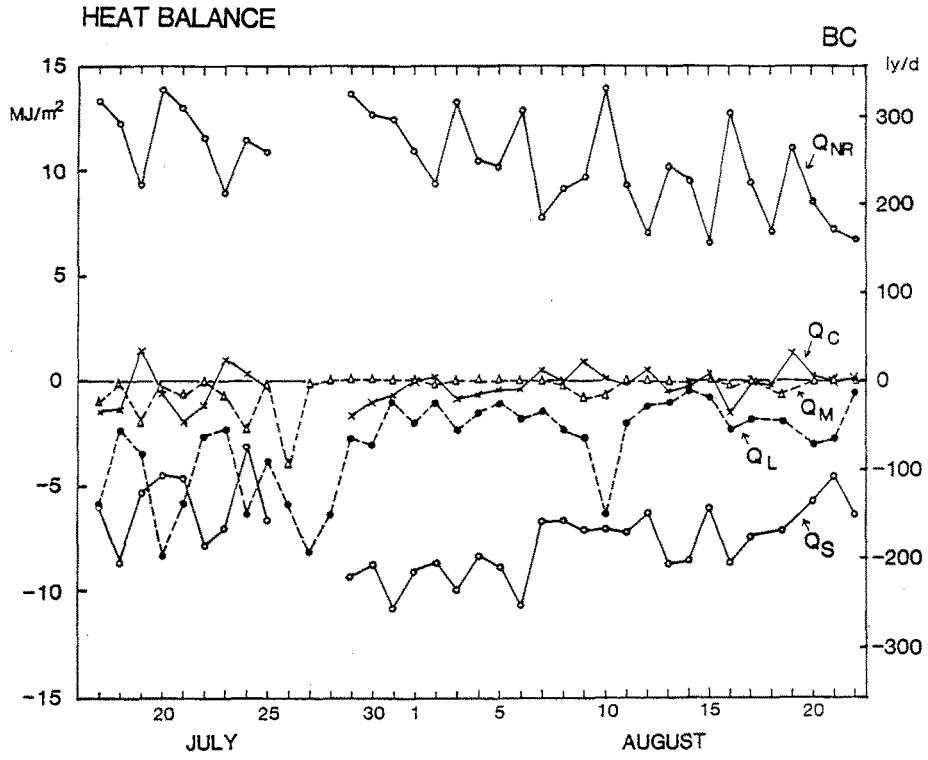

Fig. 14. Heat fluxes on a ground surface at BC.

The water and heat balances at BC seem to be strongly dependent on the moisture condition of the ground, which is primarily dependent on the amount of precipitation. Such characteristics of the water and heat balances at BC are probably due to the following facts.

1) Low total precipitation amount and low precipitation intensity.
2) Precipitation occurs as snow.
3) Dry ground surface.

5. Discussion

Evaporation from the surface was remarkably large and played an important role in the heat and mass balance on both the glacier and ground surfaces in this region. Several reasons for this are considered below.

The first reason is that the glacier is located in an arid climate area. According to humidity observation (Ohata *et al.*, 1989), vapor pressure was, on the average, smaller than the saturated vapor pressure at 0°C and occasionally became less when dry air mass moved in from the Taklimakan Desert.

The second reason is the low atmospheric pressure of the high altitude: below 500 mb on the glacier. Generally, the vapor flux is proportional to the gradient of specific humidity (ratio of vapor pressure to atmospheric pressure). Since the atmospheric pressure is below 500 mb on the Ice Cap (above 5800m), the specific humidity and its gradient on the melting snow surface are twice as large as the ones at sea-level pressure, and the evaporation is expected to be double.

The third reason is the strong solar radiation (*e.g.* about 38 MJ/m²d at the end of July). Usually water vapor flux was estimated by vapor pressure gradient, wind speed and bulk transfer coefficient based on the eddy diffusion theory (*e.g.* Male, 1980). Schmidt (1972) considered solar radiation as an additional energy source for sublimation of blowing snow particles. This conception can be extended to the evaporation of melting snow; strong solar radiation on this altitude may enhance evaporation, and therefore the evaporation may be large in daytime.

Ageta *et al.* (1989) observed an altitudinal dis-

tribution of mass balance on the Chongce Ice Cap in the same period as our observation. To extend this mass-balance distribution to other seasons, heat balance components should be estimated from limited meteorological factors at BC or other meteorological station. So far, the empirical formulas for the components have usually been obtained at the standard atmospheric pressure, and they cannot apply to conditions at low pressure at high altitude (above 5000m). The effect of the high altitude on the estimate of the heat balance components should be taken into account by the following reasons.

For the downward long-wave radiation, $Q_{RL}\downarrow$, the most widely quoted expression is that of Brunt (1952), which has the form

$$Q_{RL}\downarrow = \sigma T^4(a+b\sqrt{e}), \tag{6}$$

where σ is the Stephan-Boltzmann constant, T is the absolute air temperature, e is the vapor pressure, and a and b are empirical parameters. On the other hand, Brutsaert (1975) has suggested a means of estimating the long-wave radiation which takes into consideration temperature and humidity profile above the surface. Assuming a constant temperature lapse rate, -0.006°C/m, he obtained an expression for $Q_{RL}\downarrow$ at the standard atmospheric pressure, 1000 mb:

$$Q_{RL}\downarrow = 0.642\ (e/T)^{1/7}\sigma T^4. \tag{7}$$

Marks (1979) has modified this equation for the use in the alpine areas on the assumption that relative humidity is constant with height and temperature variations with height follow the standard lapse rate. This method can be applied to the high-altitude area of our observation.

For the the calculations of sensible heat flux, Q_S, and latent heat flux, Q_L, the bulk transfer coefficient at high altitude must be different from that at the standard atmospheric pressure. Many investigators have examined the bulk transfer expressions:

$$\begin{aligned} Q_S &= D_A\ u_a(T_a - T_0) \\ Q_L &= D_E\ u_a(e_a - e_0), \end{aligned} \tag{8}$$

where D_A and D_E are bulk transfer coefficients, e is the vapor pressure, and the subscripts a and 0 denote the measurement height and surface condition respectively. However, most of the experimental values of the transfer coefficient are obtained for the standard atmospheric pressure. For the low pressure at high altitude, we should use the original form of turbulent flux:

$$\begin{aligned} Q_S &= \rho C_p k^2 (K_A/K_M)(u_b - u_a)(T_b - T_a)/\ln^2(b/a), \\ Q_L &= \rho L_v k^2 (K_E/K_M)(u_b - u_a)(q_b - q_a)/\ln^2(b/a), \end{aligned} \tag{9}$$

where ρ is the air density, C_p the specific heat at constant pressure, L_v the latent heat of vaporization, k the von Karman constant, q the humidity ratio. The subscripts a and b denote the measurement heights. K_M, K_A and K_E are the eddy diffusivity for sensible heat, water vapor and momentum flux. In these expressions, ρ, K_M, K_A and K_E are functions of atmospheric pressure.

For the calculation of heat balance components on a glacier at a high altitude, these effects of the high altitude (low pressure) on the components should be taken into account.

6. Concluding remarks

The heat and water balances were examined on a glacier surface and on a ground surface at the Chongce Ice Cap in the West Kunlun Mountains in summer, 1987.

On a glacier surface at the terminus of the Chongce Ice Cap (5850m a.s.l.), the latent heat flux by evaporation was much larger than the heat for snow melting, and the evaporation from the surface was the main component for the outgoing mass flux.

The evaporation rate on the glacier surface showed a good correlation with air temperature, not with vapor pressure or wind speed, while the melting rate was correlated with the solar radiation, not with air temperature. From the recursive relations, the mean evaporation rate during July 23 and August 18 was estimated as 1.36mm/d, and the mean melting rate was 3.52mm/d.

On a ground surface (5260m a.s.l.), the total amount of evaporation from July 17 to August 22 was 51.6mm and that of precipitation was 52.3mm; most of the precipitation was evaporated and no water was percolated into the ground. The evaporation rate was 1.36mm/d same as that on the glacier surface.

The large evaporation is considered to be owing to the arid climate, the low atmospheric pressure at high altitude, and the strong solar radiation in this area.

The effects of high altitude on the heat balance components are a future subject of the heat and water balances on glaciers and ice caps at high altitudes.

Acknowledgments

We would like to express our appreciation to the members of the Sino-Japanese Joint Glaciological Expedition to the West Kunlun Mountains, 1987, for their generous help to our works. This research was financially supported by a Grant-in-Aid for Scientific Research from the Ministry of Education, Science and Culture, Japanese Government. (No. 62041043, 63043030)

References

Ageta, Y., Zhang, W. and Nakawo, M. (1989): Mass balance studies on Chongce Ice Cap in the West Kunlun Mountains. Bulletin of Glacier Research, **7**, 37–43.

Brunt, D. (1952): Physical and dynamical meteorology.London and New York, Cambridge Univ. Press.

Brutsaert, W. (1975): On a derivable formula for long-wave radiation from clear skies. Water Resources Research, **11**, 742–744.

Male, D. H. (1980): The seasonal snow cover. Dynamics of snow and ice masses (Colbeck S., C. eds.), New York, Academic Press, 305–395.

Marks, D. (1979): An atmospheric radiation model for general alpine application. Proc. Modeling of snow cover runoff, U. S. Army CRREL, 167–178.

Ohata, T., Takahashi, S. and Kang, X. (1989): Meteorological conditions of the West Kunlun Mountains in summer of 1987. Bulletin of Glacier Research, **7**, 67–76.

Schmidt, R. A. (1972): Sublimation of wind–transported snow. U.S., For. Serv., Res. Pap. RM **90**, 24 p.

Zhang, Z. and Jiao, K. (1987): Modern glaciers on south slope of the West Kunlun Mountains 1985. Bulletin of Glacier Research, **5**, 85–91.